

# MOBILE ACCELERATOR BASED ON IRONLESS PULSED BETATRON FOR DYNAMIC OBJECTS RADIOGRAPHY

V. A. Fomichev\*, A. A. Chinin, S. G. Kozlov, Yu. P. Kuropatkin, V. I. Nizhegorodtsev,  
I. N. Romanov, K. V. Savchenko, V. D. Selemir, O. A. Shamro, E. V. Urlin,  
FSUE "RFNC-VNIIEF", 607190 Sarov, Russia

## Abstract

The paper concerns a mobile accelerator based on the ironless pulsed betatron. The accelerator has a possibility to obtain up to three frames in a single pulse and is aimed to radiograph dynamic objects with a large optical thickness. The block diagram of the accelerator, the temporal diagram of its separate systems operation and oscillograms of the betatron output parameters are provided. The testing powering in a single-frame mode was carried out in 2018. The capacitance of the storage of the betatron electromagnetic pulsed power system that defines the electron beam energy was equal to 1800  $\mu\text{F}$ . The following test results have been obtained. The thickness of the lead test object examined with X-rays reached 140 mm at 4 m from the tantalum target of the betatron. The full width of the output gamma pulse at half maximum in a single-frame mode was equal to 120 ns; the dimension of the radiation source was  $3 \times 6 \text{ mm}^2$ ; the dimension of the tantalum target was  $6 \times 6 \text{ mm}^2$ . The application of these accelerators within the radiographic complex enables the optimization of the hydrodynamic experiments geometry resulting in the increase of the test efficiency.

## INTRODUCTION

A broad spectrum of the experimental tasks concerning the dynamic processes investigation in the optically dense matter requires the development of powerful sources of pulsed radiation with the optimal spectral composition.

Depending on the method of the particles acceleration the sources of radiation for dynamic objects radiography can be divided into linear [1] and cyclic ones [2]. Both methods of acceleration have their own advantages and disadvantages, and the appropriateness of their application is defined according to the certain task.

The ironless pulsed compact betatrons of the BIM type [3] have been used in FSUE "RFNC-VNIIEF" and FSUE "RFNC-VNIITF" for a long time in radiographic complexes to conduct hydrodynamic investigations.

To reduce expenses and optimize the process of hydrodynamic experimentation, FSUE "RFNC-VNIIEF" began to apply the concept of using mobile radiographic complexes (MRC) [4]. MRC consists of mobile cyclic accelerators (MCA) [5], an explosion-proof chamber (EPC) with a test object, X-ray collimation and shadow image recording systems. One EPC can be maintained by several MCAs. Figure 1 presents one of the options of the hydrodynamic experiment that allows obtaining up to three frames at one test.

\* mailbox@ntc.vniief.ru



Figure 1: Photo of a single-beam three-frame mobile radiographic complex: 1 – accelerator unit; 2 – pulsed power unit of the betatron electromagnet; 3 – EPC; 4 – X-ray collimation system; 5 – shadow image recording system.

## DESCRIPTION OF THE MOBILE ACCELERATOR

MCA based on the betatron of the BIM type consists of two units: an accelerator unit (AU) and a pulsed power unit of the betatron electromagnet (PPUBE). The units are located in the vans.

There are accelerator elements of the radiographic facility in the van of the accelerator unit. In the other van there is a pulsed power system of the betatron electromagnet and technological equipment. The connection between the units and the external automated control system is performed with the use of the cable and fiber-optic lines.

The block diagram of the MCA BIM is shown in Figure 2. The MCA BIM consists of a betatron, injector, high-voltage supply system, low-voltage and high-voltage synchronization system, automated control system, data gathering and processing system of the radiation source output parameters, electron beam dumping system ("low" and "fast" dumping), technological and life support systems.

The electron acceleration in the betatron is realized by the vortex electric field that appears because of the capacitive storage discharge through the electromagnet coils. Hereby, the magnetic field changes by the sine law:  $B(t) = B_0 \sin(\Omega t)$ , where  $\Omega = 1/(LC)^{1/2}$  is a circuit cyclic frequency ( $L$  and  $C$  are circuit inductance and its capacity); and  $B_0 = KI_{\max}$  is a field in the equilibrium orbit at the peak current of the electromagnet  $I_{\max}$  (here,  $K$  is a conversion coefficient). The correct selection of the electromagnet coils geometry makes the magnetic field inductance change synchronically with the acceleration. It allows holding an electron beam in the equilibrium orbit. The high-voltage electromagnet power unit is switched on firstly, forming the signal "0 field".

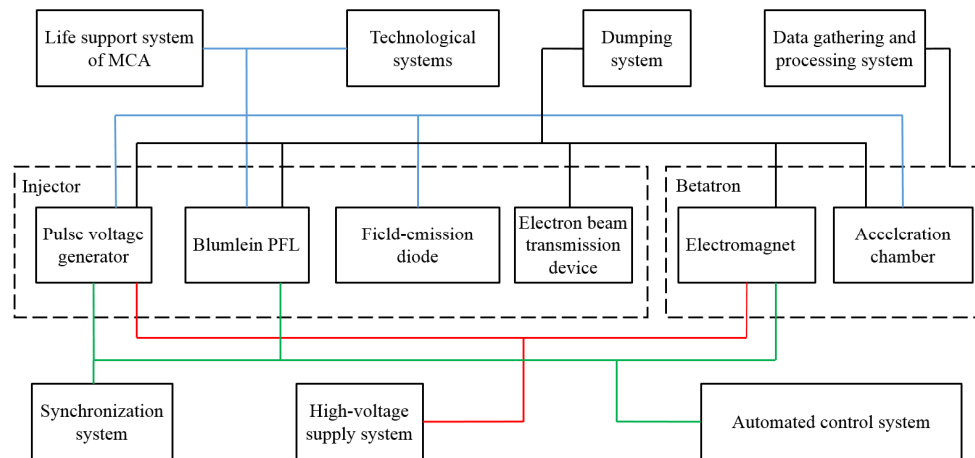


Figure 2: The block diagram of the MCA BIM.

Thereafter the time reading of facility systems turn-ons starts (pulse voltage generator, Blumlein pulse forming line, electron beam transmission device, etc.). The electron beam is generated and preliminary accelerated in the injector. In this case it is the 1.5 MeV accelerator of the direct action. The injector operates in the following way. The Blumlein pulse forming line (PFL) is charged at the same time as pulse voltage generator (PVG) is discharged. An operating voltage pulse is formed in the PFL after a PFL gas discharger actuation. Then this pulse is transmitted through the intermediate discharger to the field-emission diode. The field-emission diode is the unit where an electron beam with a current amplitude of 2 kA and a pulse width at half maximum of 10 ns is generated. The transmission and focusing of the electron beam from the field-emission diode to the betatron is performed with the use of the electron beam transmission device that contains two magnetic lenses. These magnetic lenses are powered from high voltage power supply units. A beam injection into the betatron occurs at the moment  $t_{inj}$ , when the magnetic field in the equilibrium orbit reaches the value that is defined by the ratio:  $B = B_0 \sin(\Omega t_{inj}) = E/(300R_0)$ . Here,  $R_0$  is a radius of the equilibrium orbit;  $E$  is the electron beam energy. Hereby, an injection moment can be defined by the equation:  $t_{inj} = \arcsin(E/(300B_0R_0))/\Omega$ . Electrons accelerated by the vortex electric field till the peak energy are dumped to the tantalum target because of the betatron magnetic field perturbation. Special dumping coils are responsible for the magnetic field perturbation; they are located in the electromagnet and are powered from the low and fast dumping generators.

## RESULTS OF TESTING POWERING 2018

The testing powering of the MCA BIM was carried out in 2018. The value of the capacitive storage of the pulsed power system of the betatron electromagnet was 1800  $\mu\text{F}$  as opposed to previous years [6]. All the accelerator systems operated in the normal mode during the testing powering of the MCA BIM. The temporal diagram of the accelerator subsystems operation at the testing powering is shown in Figure 3.

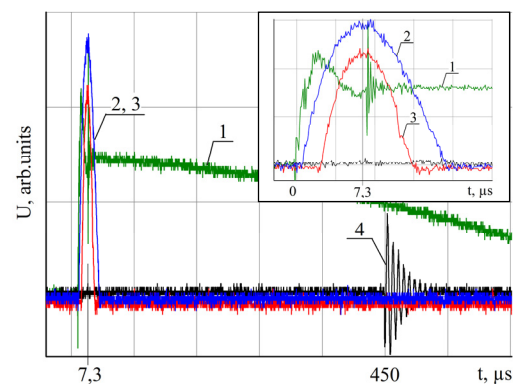


Figure 3: The temporal diagram of the accelerator subsystems operation: 1 – signal from the sensor «0 field»; 2 – signal of the current pulse in the solenoid of the electron beam transmission device; 3 – signal of the current pulse in the magnetic lens of the transmission device; 4 – signal of the current pulse at the response of a fast dumping generator.

The typical oscillograms of the betatron output parameters are presented in Figure 4.

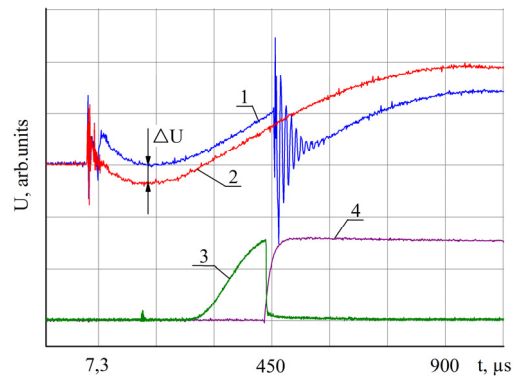


Figure 4: Oscillograms of the signals from the sensors of the MCA BIM: 1 – signal from the Rogowski coil without electrons current in the chamber; 2 – signal from the Rogowski coil with electrons current in the chamber; 3 – signal from the optic sensor of a synchrotron radiation; 4 – intensity level of the bremsstrahlung.

The electron beam current circulating in the betatron orbit was estimated by means of the Rogowski coil. The coil was located on the external surface of the acceleration chamber and orthogonally to the direction of the electron beam motion. The signals difference of  $\Delta U$  from the Rogowski coil was measured by the oscillograms (diagrams 1 and 2 in Figure 4) with and without electrons current in the chamber. Then according to the method [7], the difference of  $\Delta U$  was recalculated into the electron beam current in the betatron chamber. In this case the value of the electron beam current was close to 80 A. The diagram 3 in the Figure 4 is a signal from the optic sensor of the electron beam synchrotron radiation in the betatron chamber. The diagram 4 in Figure 4 is a signal from the sensor of the bremsstrahlung intensity level.

The X-ray radiography of the lead test object was carried out to estimate the transmission ability of the radiation source. The test object was a lead parallelepiped with holes. Four lead plates were placed in front of the test object. Therefore, the minimum thickness of the lead was 60 mm with further growing of the thickness every 10 mm. The shadow image recording of the lead test object and radiation source was conducted with the use of the system ImagePlate and the scanner CRX-30. The photo of the assembly for the transmission ability definition and the X-ray picture of the lead test object are provided in Figure 5. The maximum thickness of the X-rayed lead test object reached 140 mm at 4 m from the betatron tantalum target.

The camera obscura was used to estimate the dimension of the bremsstrahlung source. The X-ray photograph of the radiation source and its densitogram are presented in Figure 6.

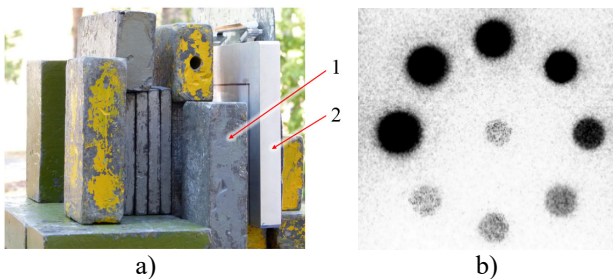


Figure 5: a) The photo of the assembly for the transmission ability definition of the MCA BIM: 1 – test object; 2 – ImagePlate cassette; b) X-ray picture of the lead test object.

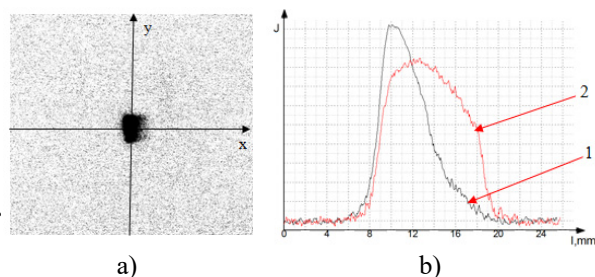


Figure 6: a) The X-ray picture of the radiation source; b) densitogram of the radiation source: 1 – along the axis X; 2 – along the axis Y.

The results analysis showed that in the experiment geometry the radiation source dimension is  $3 \times 6 \text{ mm}^2$  (full width at half maximum of the densitogram diagrams) with the dimension of the tantalum target as  $6 \times 6 \text{ mm}^2$ . The betatron chamber design allows changing the tantalum target dimension according to the experiment tasks. Also, the conducted investigations demonstrated that the reduction of the target dimension by two times causes the output radiation intensity decrease by 15-20%.

A scintillator detector based on the “stilbene” was used to measure the length of the bremsstrahlung pulse. A typical oscillogram of the  $\gamma$ -pulse signal from the detector is presented in Figure 7. The full width of the  $\gamma$ -pulse at half maximum in a single-frame mode was 120 ns.

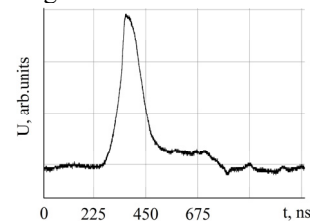


Figure 7: Oscillogram of the  $\gamma$ -pulse signal from the scintillator detector.

The MCA BIM testing is going to be continued in 2019; and there are plans to achieve operational parameters in a three-frame mode.

## CONCLUSION

The testing powering of the MCA BIM showed that the thickness of the X-rayed lead test object was 140 mm at 4 m from the tantalum target with the dimension of  $6 \times 6 \text{ mm}^2$  at the capacitance of the betatron electromagnet pulsed power system equal to 1800  $\mu\text{F}$ . The full width of the output gamma pulse at half maximum in a single-frame mode was 120 ns. The dimension of the radiation source at the geometry of the testing powering was  $3 \times 6 \text{ mm}^2$ .

## REFERENCES

- [1] A. W. Chao, “Accelerators for high intensity beams”, in *Reviews of accelerators science and technology*, W. Chou, Ed. Singapore: World Scientific, vol. 6, 2013, pp. 126-129.
- [2] V. A. Komrakov *et al.*, “Radiography”, in *Nonperturbative diagnostic techniques of fast processes*, A. L. Mikhailov, Ed. Sarov: RFNC-VNIIEF, 2015, pp. 112-114 (in Russian).
- [3] Yu. P. Kuropatkin *et al.*, “Uncored betatron BIM-M a source of bremsstrahlung for flash radiography”, *11<sup>th</sup> IEEE International PPC*, vol. 2, 1997, pp. 1669-1673.
- [4] D. I. Zenkov *et al.*, “Mobile X-ray complexes based on ironless pulsed betatrons”, in *Proc. of Conf. XVIII Khariton's Topical Scientific Readings*, vol. 2, 2016, pp. 233-236.
- [5] D. I. Zenkov *et al.*, “Mobile radiographic complex and betatron type radiation source for radiographic complex”, Patent 2548585 C1 RU MPK G03B 42/02, 2015.
- [6] Yu. P. Kuropatkin *et al.*, “Mobile cyclic accelerator based on ironless pulsed betatron. Results of testing powering”, *IOP Conf. Series: Mat. Sc. and Eng.*, vol. 366, p. 012049, 2018.
- [7] A. Grenaderov, “Device to measure the current in betatron”, *Dev. and tech. of exp.*, vol. 5, pp. 55-57, 1989 (in Russian).